Identification of multi-phonon γ-vibrational bands in odd-Z ^{105}Nb

H. J. Li (李红洁),[1] S. J. Zhu (朱胜江),[1,2,*] J. H. Hamilton,[2] A. V. Ramayya,[2] J. K. Hwang,[2] Y. X. Liu (刘艳鑫),[3] Y. Sun (孙扬),[4] Z. G. Xiao (肖志刚),[1] E. H. Wang,[2] J. M. Eldridge,[2] Z. Zhang (张钊),[1] Y. X. Luo,[2,5] J. O. Rasmussen,[5] I. Y. Lee,[5] G. M. Ter-Akopian,[6] A. V. Daniel,[6] Yu. Ts. Oganessian,[6] and W. C. Ma[7]

[1]*Department of Physics, Tsinghua University, Beijing 100084, People's Republic of China*
[2]*Department of Physics, Vanderbilt University, Nashville, Tennessee 37235, USA*
[3]*School of Science, Huzhou Teachers College, Huzhou 313000, People's Republic of China*
[4]*Department of Physics, Shanghai Jiao Tong University, Shanghai 200240, People's Republic of China*
[5]*Lawrence Berkeley National Laboratory, Berkeley, California 94720, USA*
[6]*Flerov Laboratory for Nuclear Reactions, JINR, 141980 Dubna, Russia*
[7]*Department of Physics and Astronomy, Mississippi State University, Mississippi State, Mississippi 39762, USA*

(Received 27 June 2013; revised manuscript received 11 August 2013; published 13 November 2013)

Background: The odd-Z ^{105}Nb nucleus is located in the $A = 100$ neutron-rich region. The study of multi-phonon vibrational band structures is important for understanding nuclear structure in this region.
Purpose: To search for multi-phonon γ-vibrational bands in ^{105}Nb.
Methods: The high spin states of ^{105}Nb have been studied by measuring the prompt γ rays emitted in the spontaneous fission of ^{252}Cf. The data analysis is carried out using triple- and four-fold γ coincidence methods.
Results: A new level scheme of ^{105}Nb is established. The yrast band has been confirmed, and three new collective bands have been identified. Compared with previous results, a total of 14 new levels and 36 new γ transitions are observed. Two bands built on 625.9 keV and 1231.9 keV levels are proposed as one-phonon- and two-phonon γ-vibrational bands, respectively. The evidences for supporting assignments of the multi-phonon γ-vibrational bands have been discussed. Triaxial projected shell model calculations for the γ-vibrational band structures are found in good agreement with the experimental data, thus further supporting the γ-vibrational interpretations for the experimental results in ^{105}Nb.
Conclusions: The one-phonon- and two-phonon γ-vibrational bands have been identified in ^{105}Nb. Our results provide new data to systematically understand the characteristics of the multi-phonon γ-vibrational bands in the $A = 100$ neutron-rich region.

DOI: 10.1103/PhysRevC.88.054311 PACS number(s): 21.10.Re, 23.20.Lv, 27.60.+j, 25.85.Ca

I. INTRODUCTION

In recent years, following the development of large and efficient γ-ray multi-detector arrays, experimental investigations of the multi-phonon γ-vibrational bands in $A = 100$ neutron-rich nuclei have made remarkable progress. So far, multi-phonon γ-vibrational bands were identified up to two-phonon bands. In even-even nuclei, the observed multi-phonon γ-vibrational bands include a ground state [zero-phonon γ-vibrational (0γ)] band, a one-phonon γ-vibrational (1γ) band based on 2^+ level, and a two-phonon γ-vibrational (2γ) band built on 4^+ level. In the $A = 100$ neutron-rich region, such multi-phonon γ-vibrational bands have been identified in several even-even nuclei, such as in ^{104,106,108}Mo [1–6] and ^{108,110,112,114}Ru [7–10]. For odd-A nuclei, the multi-phonon γ-vibrational bands involve the coupling of the single-particle motion, collective vibration, and collective rotation. Multi-phonon γ-vibrational bands would include a quasiparticle band with the band-head quantum number K (0γ band), a 1γ band built on $K + 2$ level, and a 2γ band built on $K + 4$ level. Recently, such multi-phonon γ-vibrational bands have been identified in odd-A ^{105}Mo [11], ^{103}Nb [12], ^{107}Tc [13], and ^{109}Tc [14] by our collaboration. These are the only four such bands discovered in odd-A nuclei until now. Several theoretical models have also been developed to successfully describe the multi-phonon γ-vibrational bands, for example, the triaxial projected shell model approach [10,15], and the particle vibration coupling model [16].

The ^{105}Nb with $Z = 41$ and $N = 64$ is located in the $A = 100$ neutron-rich region. Searching for multi-phonon γ-vibrational bands in this nucleus is important for systematically understanding the structural characteristics in this region. By using spontaneous fission experiments, the ground state band in ^{105}Nb was identified in Ref. [17] and then expanded in Ref. [18]. In this paper, we reinvestigated the level structure of ^{105}Nb. Many new levels and transitions are observed, and the 1γ and 2γ bands have been proposed. Total Routhian surface and triaxial projected shell model calculations were carried out. These calculations support our 1γ and 2γ assignments.

II. EXPERIMENT AND RESULTS

As ^{105}Nb is located in the $A = 100$ neutron-rich region, to study its high spin states is difficult using the usual heavy-ion fusion-evaporation reactions. A practical method is to measure the prompt γ rays of spontaneous fission or particle induced fission from heavy nuclei by using a large detector array [19]. The experiment was carried out at Lawrence Berkeley National Laboratory. A ^{252}Cf source, with the strength of about 60 μCi, was sandwiched between two Fe foils with the

*zhushj@mail.tsinghua.edu.cn

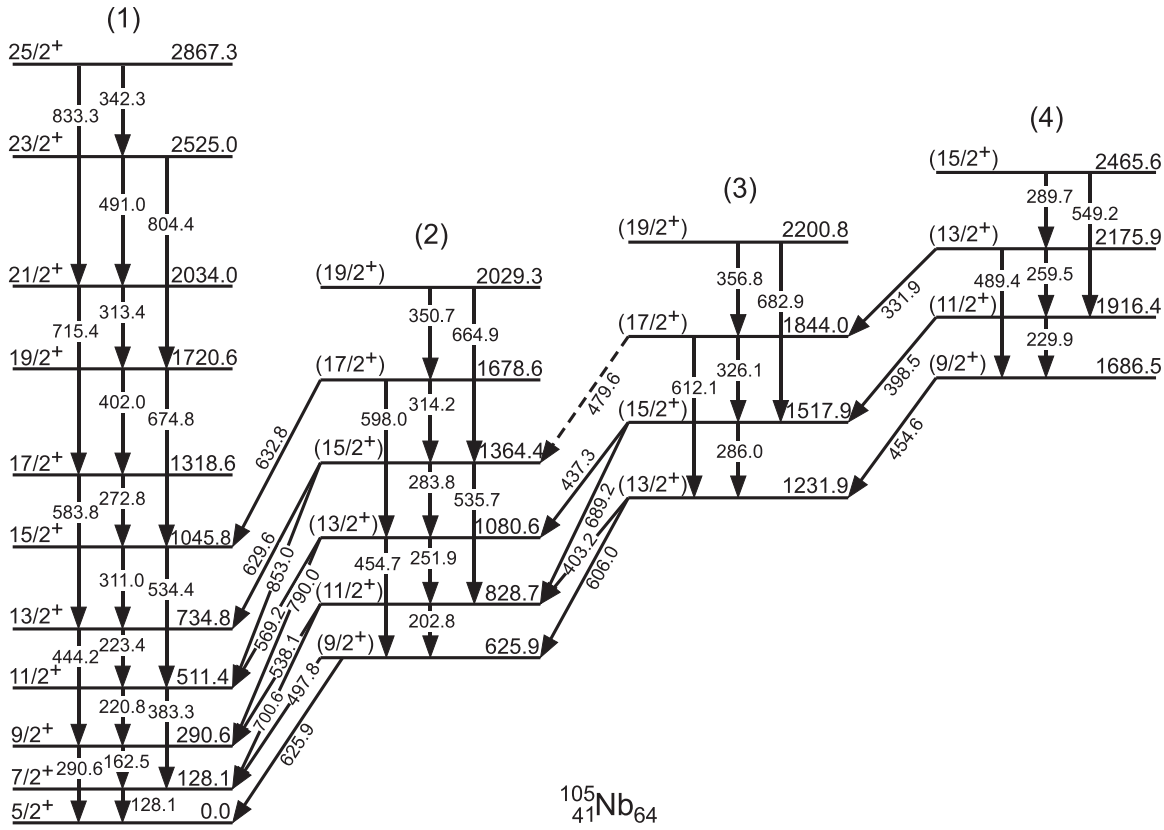

FIG. 1. The level scheme of ^{105}Nb identified in the present paper.

thickness of 10 mg/cm^2. Then they were placed in the center of the Gammasphere detector array, which consisted of 101 Compton-suppressed Ge detectors in this experiment. A total of 5.7 $\times$ 10^{11} triple- or higher-fold coincidence events were collected. A γ-γ-γ coincidence matrix (cube) and a γ-γ-γ-γ coincidence matrix (hypercube) were constructed. The data analysis is carried out with the triple- and four-fold γ coincidence methods using the RADWARE software package [20].

Through coincidence data analysis, a new level scheme of ^{105}Nb is established as shown in Fig. 1. The collective band structures have been labeled on the top of the bands with the numbers (1)–(4). The γ rays attributed to ^{105}Nb are listed in Table I, along with the relative transition intensities, and the assignments of spin and parity (I^{π}). The γ transition intensities have been normalized to that of the 128.1 keV ($7/2^+ \rightarrow 5/2^+$) γ ray. Energies and intensities of transitions which have similar energies were obtained from double gates which isolated each transition, for example, the 289.7 and 290.0 keV transitions were seen separately in the 625.9 and 606.0, and 220.8 and 311.0 keV double gated spectra, respectively. In the present paper, a total of 14 new energy levels and 36 new γ transitions are observed in ^{105}Nb, in addition to those found in our previous work.

As ^{105}Nb is a very neutron-rich nucleus, its fission yield is low in the spontaneous fission of ^{252}Cf. It is difficult to identify the new side bands in this nucleus. However, through complex γ-γ-γ coincidence analysis, we have clearly identified the new γ transitions belonging to ^{105}Nb. As examples, we present several double-gating spectra in the present data analysis. Figure 2 shows a γ-ray spectrum obtained by summing double gates on the 128.1 and 162.5 keV γ transitions, and 128.1 and 220.8 keV γ transitions. In this spectrum, one can see all the γ transitions above the 128.1 keV level in band (1), except for the 383.3 keV γ ray, most of the γ transitions in bands (2)—(4), and some linking transitions between these bands. The 202.7, 230.6, and 276.4 keV γ transitions in this figure are contaminating γ rays from ^{101}Y [18]. In Fig. 3, a coincidence spectrum is obtained by summing double gates on the 128.1 and 700.6 keV γ transitions, and 128.1 and 538.1 keV γ transitions. From this spectrum, one can see the γ transitions above the 828.7 keV level in band (2) along with those in bands (3) and (4), as well as some linking γ rays between bands (2) and (3), and between bands (3) and (4). Figures 4(a) and 4(b) are generated by double gates on the 128.1 and 606.0 keV γ transitions, and by triple gates on the 128.1, 497.8, and 606.0 keV γ transitions, respectively. Here one can see all the γ transitions in bands (3) and (4), and the linking transitions between bands (3) and (4), as well as the 497.8 keV linking γ transition between bands (1) and (2). On the other hand, as shown in Figs. 4(a) and 4(b), the spectrum from the hypercube has approximately a factor of 10 fewer events than the triple-coincidence cube. However, the hypercube reduced the contamination and increased the peak to background ratio significantly. In spontaneous fission, a pair of correlated partners is produced. By gating on known γ rays in an isotope, one expects to see some transitions in

TABLE I. The energies, relative intensities, and spin and parity assignments of the γ transitions and levels in ^{105}Nb. The $*$ denotes the γ transitions newly identified in this paper compared with the results reported in Ref. [18].

E_γ (keV)	Intensity (%)	E_i (keV)	E_f (keV)	Assignment
128.1(1)	100	128.1	0.0	$7/2^+ \rightarrow 5/2^+$
162.5(1)	51.3(12)	290.6	128.1	$9/2^+ \rightarrow 7/2^+$
$*$202.8(2)	15.4(5)	828.7	625.9	$(11/2^+) \rightarrow (9/2^+)$
220.8(1)	44.0(9)	511.4	290.6	$11/2^+ \rightarrow 9/2^+$
223.4(2)	19.6(5)	734.8	511.4	$13/2^+ \rightarrow 11/2^+$
$*$229.9(2)	6.0(2)	1916.4	1686.5	$(11/2^+) \rightarrow (9/2^+)$
$*$251.9(1)	11.5(6)	1080.6	828.7	$(13/2^+) \rightarrow (11/2^+)$
$*$259.5(2)	4.4(2)	2175.9	1916.4	$(13/2^+) \rightarrow (11/2^+)$
272.8(2)	7.2(2)	1318.6	1045.8	$17/2^+ \rightarrow 15/2^+$
$*$283.8(1)	9.3(4)	1364.4	1080.6	$(15/2^+) \rightarrow (13/2^+)$
$*$286.0(1)	9.0(3)	1517.9	1231.9	$(15/2^+) \rightarrow (13/2^+)$
$*$289.7(2)	2.0(1)	2465.6	2175.9	$(15/2^+) \rightarrow (13/2^+)$
290.6(2)	13.5(7)	290.6	0.0	$9/2^+ \rightarrow 5/2^+$
311.0(2)	12.3(4)	1045.8	734.8	$15/2^+ \rightarrow 13/2^+$
313.4(2)	1.4(2)	2034.0	1720.6	$21/2^+ \rightarrow 19/2^+$
$*$314.2(1)	4.5(2)	1678.6	1364.4	$(17/2^+) \rightarrow (15/2^+)$
$*$326.1(1)	6.5(3)	1844.0	1517.9	$(17/2^+) \rightarrow (15/2^+)$
$*$331.9(2)	1.1(1)	2175.9	1844.0	$(13/2^+) \rightarrow (17/2^+)$
342.3(3)	<1	2867.3	2525.0	$25/2^+ \rightarrow 23/2^+$
$*$350.7(1)	1.3(1)	2029.3	1678.6	$(19/2^+) \rightarrow (17/2^+)$
$*$356.8(2)	2.2(2)	2200.8	1844.0	$(19/2^+) \rightarrow (17/2^+)$
383.3(2)	8.8(6)	511.4	128.1	$11/2^+ \rightarrow 7/2^+$
$*$398.5(2)	3.8(2)	1916.4	1517.9	$(11/2^+) \rightarrow (15/2^+)$
402.0(2)	4.7(3)	1720.6	1318.6	$19/2^+ \rightarrow 17/2^+$
$*$403.2(2)	6.0(3)	1231.9	828.7	$(13/2^+) \rightarrow (11/2^+)$
$*$437.3(3)	<1	1517.9	1080.6	$(15/2^+) \rightarrow (13/2^+)$
444.2(1)	9.8(5)	734.8	290.6	$13/2^+ \rightarrow 9/2^+$
$*$454.6(3)	16.7(5)	1686.5	1231.9	$(9/2^+) \rightarrow (13/2^+)$
$*$454.7(2)	7.4(6)	1080.6	625.9	$13/2^+ \rightarrow 9/2^+$
$*$(479.6)(5)	$\sim$	1844.0	1364.4	$(17/2^+) \rightarrow (15/2^+)$
$*$489.4(5)	2.9(2)	2175.9	1686.5	$(13/2^+) \rightarrow (9/2^+)$
491.0(2)	1.3(2)	2525.0	2034.0	$23/2^+ \rightarrow 21/2^+$
$*$497.8(1)	15.2(15)	625.9	128.1	$(9/2^+) \rightarrow 7/2^+$
534.4(2)	6.8(5)	1045.8	511.4	$15/2^+ \rightarrow 11/2^+$
$*$535.7(2)	7.6(9)	1364.4	828.7	$(15/2^+) \rightarrow (11/2^+)$
$*$538.1(2)	4.1(3)	828.7	290.6	$(11/2^+) \rightarrow 9/2^+$
$*$549.2(2)	4.3(3)	2465.6	1916.4	$(15/2^+) \rightarrow (11/2^+)$
$*$569.2(2)	3.3(1)	1080.6	511.4	$(13/2^+) \rightarrow 11/2^+$
583.8(1)	7.0(2)	1318.6	734.8	$17/2^+ \rightarrow 13/2^+$
$*$598.0(1)	5.4(3)	1678.6	1080.6	$(17/2^+) \rightarrow (13/2^+)$
$*$606.0(1)	27.7(12)	1231.9	625.9	$(13/2^+) \rightarrow (9/2^+)$
$*$612.1(4)	<1	1844.0	1231.9	$(17/2^+) \rightarrow (13/2^+)$
$*$625.9(1)	38.2(23)	625.9	0.0	$(9/2^+) \rightarrow 5/2^+$
$*$629.6(2)	1.9(1)	1364.4	734.8	$(15/2^+) \rightarrow 13/2^+$
$*$632.8(2)	1.0(1)	1678.6	1045.8	$(17/2^+) \rightarrow 15/2^+$
$*$664.9(2)	2.1(2)	2029.3	1364.4	$(19/2^+) \rightarrow (15/2^+)$
674.8(2)	2.9(2)	1720.6	1045.8	$19/2^+ \rightarrow 15/2^+$
$*$682.9(2)	1.3(1)	2200.8	1517.9	$(19/2^+) \rightarrow (15/2^+)$
$*$689.2(5)	2.3(2)	1517.9	828.7	$(15/2^+) \rightarrow (11/2^+)$
$*$700.6(2)	8.7(6)	828.7	128.1	$(11/2^+) \rightarrow 7/2^+$
715.4(2)	2.7(2)	2034.0	1318.6	$21/2^+ \rightarrow 17/2^+$
$*$790.0(4)	4.0(3)	1080.6	290.6	$(13/2^+) \rightarrow (9/2^+)$
804.4(3)	1.2(2)	2525.0	1720.6	$23/2^+ \rightarrow 19/2^+$
833.3(2)	1.0(2)	2867.3	2034.0	$25/2^+ \rightarrow 21/2^+$
$*$853.0(3)	1.4(2)	1364.4	511.4	$(15/2^+) \rightarrow (11/2^+)$

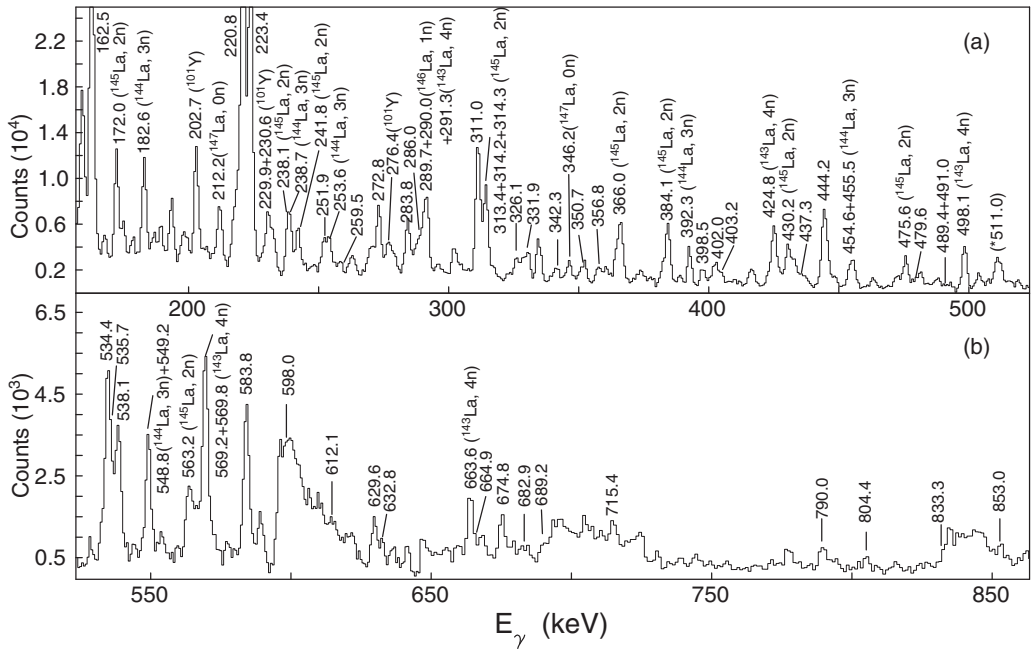

FIG. 2. Portion of the γ ray spectrum obtained by summing double gates on the 128.1 and 162.5 keV γ transitions, and 128.1 and 220.8 keV γ transitions in ^{105}Nb. The range of the energy is (a) from 157 to 523 keV, and (b) from 523 to 863 keV.

its correlated partners. The partners of ^{105}Nb in ^{252}Cf fission are ^{147}La ($0n$), ^{146}La ($1n$), ^{145}La ($2n$), ^{144}La ($3n$), and ^{143}La ($4n$) (numbers in parentheses here indicate the number of neutrons emitted after fission). In Figs. 2–4, one can see some strong partner γ transitions, in addition to the γ peaks observed in ^{105}Nb. For example, 291.3, 424.8, 498.1, 569.8, 595.1, 641.0, and 663.6 keV γ transitions in ^{143}La [21]; 182.6, 238.7, 253.6, 392.3, 455.5, and 548.8 keV γ transitions in ^{144}La [21]; 172.0, 238.1, 241.8, 314.3, 366.0, 384.1, 430.2, 475.6, and 563.2 keV γ transitions in ^{145}La [22]; 290.0 keV γ transition in ^{146}La [23]; and 212.2 and 346.2 keV γ transitions in ^{147}La [22]. The 511.0 keV γ peak labeled with (*511.0) is caused by the annihilation of electrons and positrons, and the unmarked peaks should belong to the background peaks from

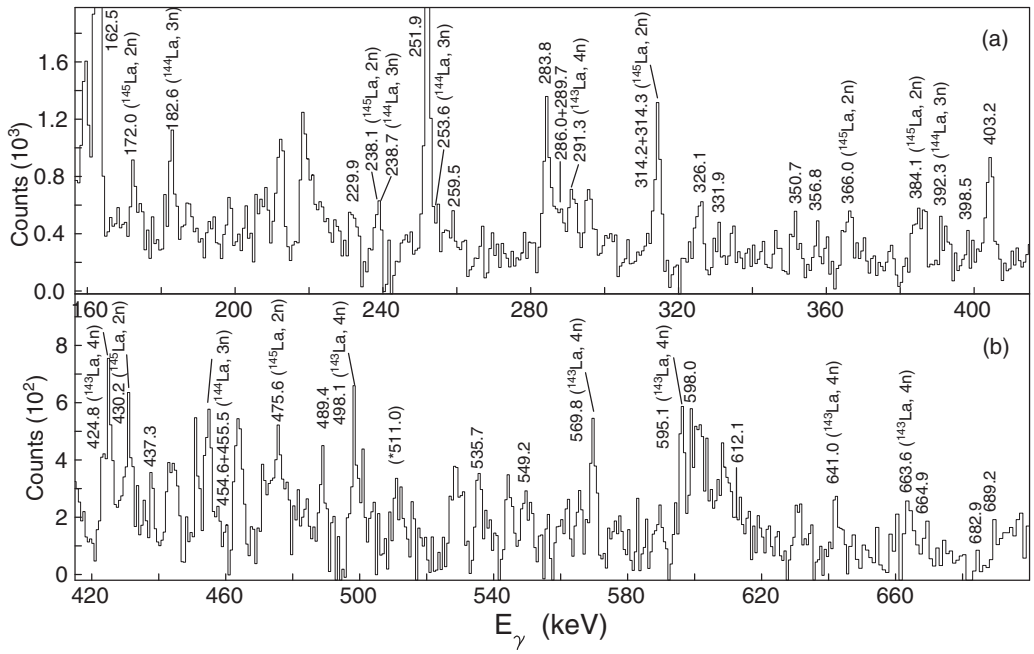

FIG. 3. Portion of the γ ray spectrum obtained by summing double gates on the 128.1 and 700.6 keV γ transitions, and 128.1 and 538.1 keV γ transitions in ^{105}Nb. The range of the energy is (a) from 155 to 415 keV, and (b) from 415 to 700 keV.

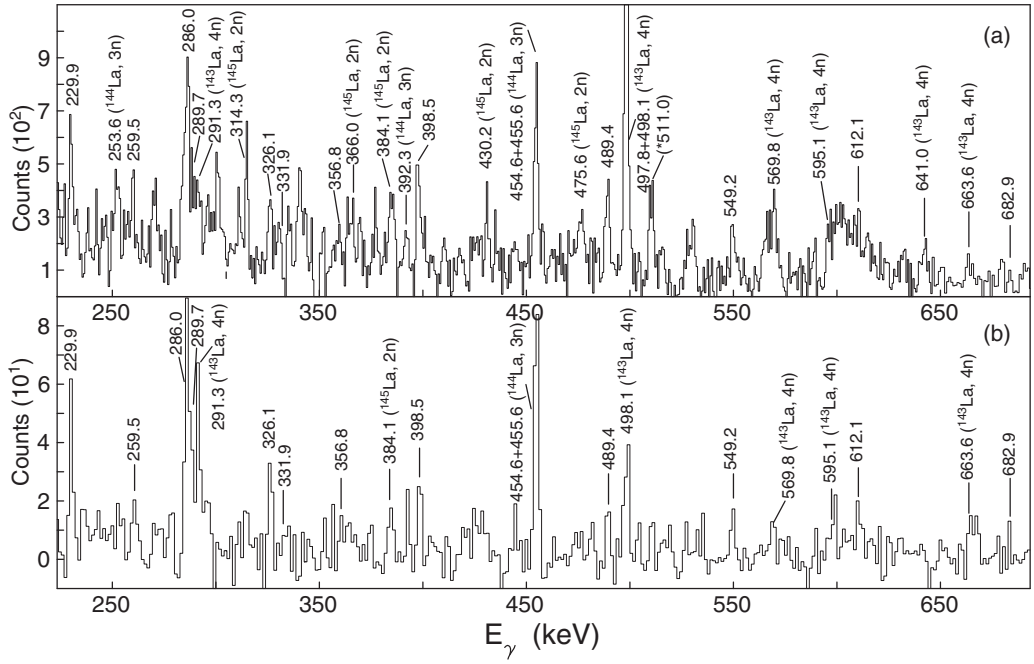

FIG. 4. Portion of the γ ray spectra of ^{105}Nb obtained by (a) double gates on the 128.1 and 606.0 keV γ transitions, and (b) triple gates on the 128.1, 497.8, and 606.0 keV γ transitions.

other fission products. Multiple double and triple gated spectra were analyzed to obtain Fig 1.

III. DISCUSSION

In the previous reports, band (1) in ^{105}Nb was identified up to $15/2^+$ level [17], and then was extended up to $25/2^+$ level [18]. We have confirmed this band in the present paper. The band head level was tentatively assigned as I^π of $5/2^+$ with $\pi 5/2^+[422]$ configuration [17,18]. By further systematic analysis based on the recent data in the neighboring isotope ^{103}Nb [12] and our triaxial projected shell model (TPSM) calculations (see the later discussions), we think that the above assignments of $5/2^+$ with $\pi 5/2^+[422]$ configuration for band (1) are right. Bands (2), (3), and (4) are newly identified in the present paper. The structures for the three bands are very similar to those observed in neighboring isotope ^{103}Nb, in which band (2) belongs to 1γ band and band (3) belongs to 2γ band. Similarly, we propose bands (2) and (3) in ^{105}Nb as 1γ and 2γ bands, respectively, as discussed below.

^{105}Nb is located in the $Z = 38$ to 40 and $N = 60$ to 62 well deformed region [19], and is expected to have large β_2 deformation. To understand the structural properties, we have carried out total Routhian surface (TRS) calculations using the cranked shell model (CSM) described in Refs. [24–26]. The calculated results are shown in Fig. 5, from which the minimum can be found at $\beta_2 = 0.339$, $\beta_4 = 0.007$, and $\gamma = 12.3^\circ$ for $\omega = 0.0$ MeV/$\hbar$. The calculated results indicate that ^{105}Nb has a large β_2 deformation and medium triaxiality. The γ value is less than that in the comparable Mo and Ru isotopes.

Band (2) is based on the excited state at 625.9 keV, which strongly decays to the $5/2^+$ and $7/2^+$ states of the ground state band (1). It is not likely for a single quasiparticle state to be built with such a high excitation energy, compared with the other single-quasiparticle bands in ^{101,103}Nb [18,23]. The observed strong linking transitions between bands (1) and (2) suggest that the levels in band (2) most probably have a positive parity. Comparing the band-head energy of band (2) in ^{105}Nb with that of the 1γ band in neighboring isotope

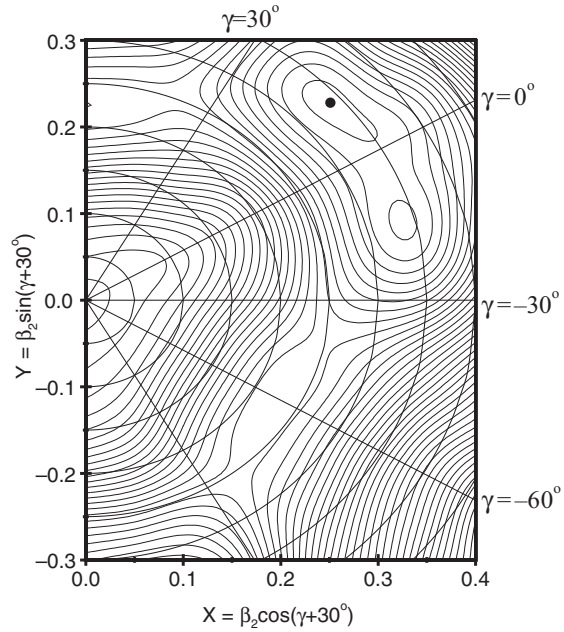

FIG. 5. Calculated polar coordinate plots of the total Routhian surface for ^{105}Nb at $\hbar\omega = 0.0$ MeV. The minimum point corresponds to $\beta_2 = 0.339$, $\beta_4 = 0.007$, and $\gamma = 12.3^\circ$.

^{103}Nb [12], and in ^{104,105,106,108}Mo [1–6,11], ^{107,109}Tc [13,14], and ^{108,110,112,114}Ru [7–10], one can see that they all have similar values. So we propose band (2) in ^{105}Nb as a 1γ band based on $9/2^+$ level. Band (3) in ^{105}Nb is built on the 1231.9 keV level. The excitation energy of the band-head level is much less than the neutron and proton pairing-gap energies, $2\Delta_n \sim 2.1$ and $2\Delta_p \sim 1.7$ MeV, in this region [1]. For this reason, band (3) should not be a three-quasiparticle band. Its band-head energy is very close to the 2γ band in ^{103}Nb and similar to the 2γ band heads in the Mo, Tc, and Ru isotopes in Table II. Indeed as shown in Fig. 7, all the proposed 1γ and 2γ levels in ^{105}Nb are very similar to those known in ^{103}Nb [12] and ^{106}Mo [1] as well as in ^{104,105,108}Mo [2,3,5,6,11] (not shown) to strongly support the ^{105}Nb assignments. In addition, the strong transitions from the 2γ to 1γ bands and the absence of even weak, higher energy same spin-parity change transitions to the yrast band clearly support the 2γ assignment since a two-phonon level should only decay to the one-phonon partners. So, we propose band (3) as a 2γ band based on a $13/2^+$ state. The I^π's of the other levels in bands (2) and (3) are tentatively assigned according to the rotational band regularity. Thus, the set of bands (1), (2), and (3) in ^{105}Nb form 0γ, 1γ, and 2γ vibrational band structures. Band (4) based on the 1686.5 keV level lies around the pairing-gap energy. There is not enough information from these experimental data to define its properties. According to the energy spacings inside the band compared with the ground band and 1γ band, the I^π for the band-head level of band (4) is tentatively assigned as $9/2^+$.

Here we give further discussions for the characteristics of the observed multi-phonon γ vibrational bands in ^{105}Nb.

In the vibrational bands of a nucleus, the g factors should be of the same magnitude [27]. The experimental value $g_K^{\rm exp}$ can be estimated from the band parameter $(g_K - g_R)/Q_0$, which is [28]

$$(g_K - g_R)/Q_0 = 0.934 E_\gamma \delta^{-1}[(I-1)(I+1)]^{-1/2}, \quad (1)$$

where g_R is the collective g factor, given by Z/A for odd-Z ^{105}Nb, Q_0 is the quadrupole moment that can be calculated with [29]

$$Q_0 = \tfrac{4}{5} Z A^{\frac{2}{3}} r_0^2 \varepsilon\left(1 + \tfrac{1}{2}\varepsilon\right), \quad (2)$$

where $\varepsilon = 0.96\beta$ and β is taken with 0.339 from the TRS result, E_γ is the cascade γ-ray energy in MeV, and $|\delta|$ is the magnitude of the $E2/M1$ mixing ratio that can be obtained from the intensity ratio of cascade I_γ and crossover $I_{\gamma'}$ transitions [28]:

$$\frac{I_\gamma}{I_{\gamma'}} = \frac{2K^2(2I-1)(1+\delta^{-2})}{[(I+1)(I-1+K)(I-1-K)]} \frac{E_\gamma^5}{E_{\gamma'}^5}. \quad (3)$$

With the intensities shown in Table I, the g_K values can be obtained as 0.96 (5) for 1γ band, and 0.93 (5) for 2γ band in ^{105}Nb. These values show that the g factors in both γ-vibrational bands indeed have the same magnitude as expected by theoretical predictions.

The 1γ and 2γ bands in a nucleus are expected to have similar inertia parameters. The inertia parameter A for a band can be extracted from the second order rotational energy formula [1]:

$$E(I,K) = E_K + A[I(I+1) - K^2] + B[I(I+1) - K^2]^2. \quad (4)$$

The values of the parameter A obtained in ^{105}Nb in the present paper are 19.5, 19.2, 19.3, and 21.4 keV for the ground state band, 1γ band, 2γ band, and band (4), respectively. These results also support our assignments.

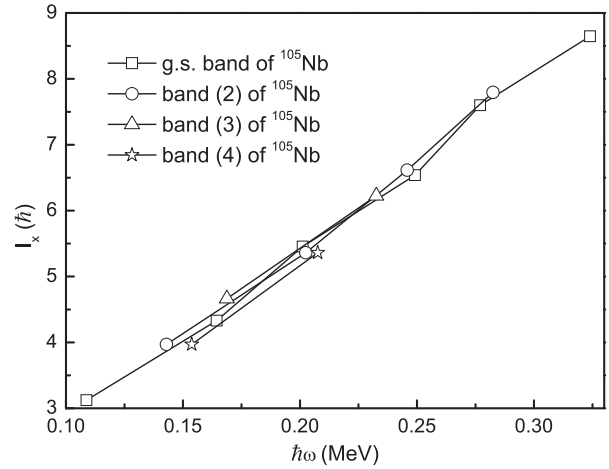

FIG. 6. The plots of the total angular momentum alignments I_x vs the rotational frequency $\hbar\omega$ for the ground state band, and bands (2)-(4) in ^{105}Nb.

The dynamical moment of inertia J_2 should have almost the same value in different multi-phonon γ-vibrational bands [30]. The J_2 values for bands (1)–(4) in ^{105}Nb can be deduced from the slopes of the angular moment I_x vs rotational frequency $\hbar\omega$ [12], which are shown in Fig. 6. The I_x is calculated as a function of $\hbar\omega$ with the formula:

$$I_x = \sqrt{(I_a + 1/2)^2 - K^2}, \quad (5)$$

where

$$I_a = (I_i + I_f)/2, \quad (6)$$

$$\hbar\omega = (E_i - E_f)/[(I+1)_x - (I-1)_x], \quad (7)$$

and K is the Ω quantum number. The similar slopes shown in Fig. 6 support the validity of the multi-phonon γ-vibrational bands in ^{105}Nb.

Another characteristic for a 2γ band is that the transitions from 2γ band to 1γ band should be collective. Also there should be no transitions to the ground band as none were found in our work. This transition collectivity can be obtained from absolute reduced transition rates $B(E2)$ values of the transitions [31]. In our paper, we cannot obtain $B(E2)$ values directly. But we can use the experimental transition intensities in Table I to calculate the $B(E2)$ ratio between two $E2$ transitions, and to obtain the relative collectivity between 1γ and 2γ bands, as done in Ref. [12]. The experimental ratios for ^{105}Nb can be calculated using the Eqs. (5) and (6) in Ref. [12] as

$$\frac{B(E2; 15/2^+_{2\gamma} \to 11/2^+_{1\gamma})}{B(E2; 11/2^+_{1\gamma} \to 7/2^+_g)} = 2.01(24) \quad (8)$$

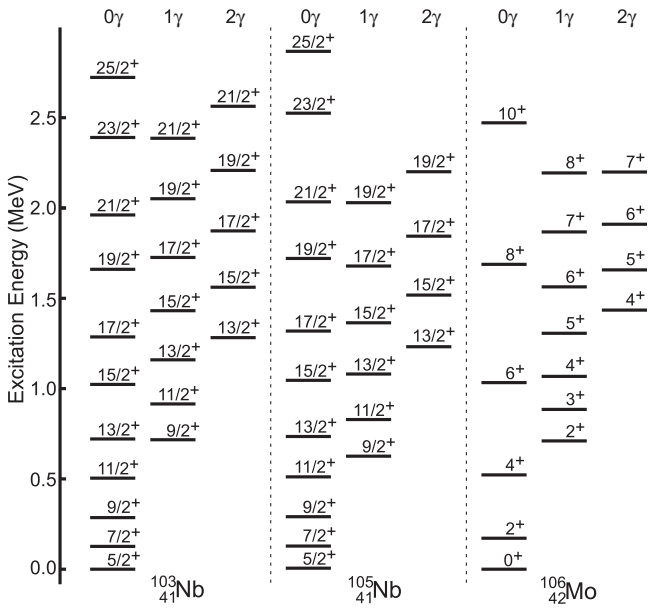

FIG. 7. The systematic comparisons for the ground-state band, 1γ band, and 2γ band of ^{105}Nb with those in ^{103}Nb [12] and ^{106}Mo [1].

and

$$\frac{B(E2;15/2^+_{2\gamma}\rightarrow 11/2^+_{1\gamma})}{B(E2;13/2^+_{1\gamma}\rightarrow 9/2^+_{g})}=1.94(25). \quad (9)$$

The corresponding theoretical ratios can be obtained using the Eqs. (2) and (3) in Ref. [1] as

$$\frac{B(E2;15/2^+_{2\gamma}\rightarrow 11/2^+_{1\gamma})}{B(E2;11/2^+_{1\gamma}\rightarrow 7/2^+_{g})}=2.59 \quad (10)$$

and

$$\frac{B(E2;15/2^+_{2\gamma}\rightarrow 11/2^+_{1\gamma})}{B(E2;13/2^+_{1\gamma}\rightarrow 9/2^+_{g})}=3.34. \quad (11)$$

The experimental ratios are close to the theoretical values, which also give support for the assignment of band (3) as a 2γ band in ^{105}Nb.

Figure 7 presents the systematic level comparisons of the 0γ, 1γ, and 2γ bands in ^{105}Nb with those in ^{103}Nb [12] and ^{106}Mo [1]. (Note the ^{104}Mo and ^{108}Mo ground, 1γ, and 2γ level energies are quite similar to ^{106}Mo.) One can see that they have very similar features. The comparisons of the band-head energies of the 0γ, 1γ, and 2γ bands and the ratios of $(E_{2\gamma}-E_{0\gamma})/(E_{1\gamma}-E_{0\gamma})$ in ^{105}Nb with those in the other nuclei in the $A=100$ neutron-rich region are shown in Table II. One can see that the energies and ratios in different nuclei show similar values. These data support the 1γ and 2γ band assignments in ^{105}Nb. The energy ratio $(E_{2\gamma}-E_{0\gamma})/(E_{1\gamma}-E_{0\gamma})$ in ^{105}Nb is 1.97, which is near to the 1.95 in ^{104}Mo and 2.02 in ^{106}Mo. These are close to the harmonic ratio 2. However, the ratios for other nuclei deviate somewhat from the harmonic ratio 2 to show anharmonic characteristics. Anharmonic values also were reported with 2.6 to 2.8 in the $A=160$ region [31–33].

Band (4) in ^{105}Nb is very similar to that observed in ^{103}Nb [12]. Since the band-head energy of 1686.5 keV is around the pairing-gap energy, band (4) could be a three-phonon γ vibrational (3γ) band or a three-quasiparticle band. Some structural characteristics of band (4) are very similar to those of the ground state band and 1γ and 2γ bands, for example, the similar inertia parameter value with 21.4 keV, and the obtained g_K value with 0.77(3). On the other hand, if the band (4) indeed belongs to 3γ band, the experimental $B(E2)$ ratios between band (4) to 2γ band and 1γ band to ground state band should have same order with those between 2γ band to 1γ band and 1γ band to ground state band. The calculated values using the observed transition intensities are

$$\frac{B(E2;11/2^+_{4}\rightarrow 15/2^+_{2\gamma})}{B(E2;11/2^+_{1\gamma}\rightarrow 7/2^+_{g})}=27.5(33) \quad (12)$$

and

$$\frac{B(E2;13/2^+_{4}\rightarrow 17/2^+_{2\gamma})}{B(E2;13/2^+_{1\gamma}\rightarrow 9/2^+_{g})}=40.5(55). \quad (13)$$

One can see that these ratios are much larger than those between 2γ to 1γ band and 1γ band to ground state band. The characteristics of this band need further studies.

To understand the multi-phonon γ-vibrational band structure in ^{105}Nb more deeply, we performed TPSM [34,35] calculations for this nucleus. The TPSM, with multi-quasiparticle (qp) configurations built in the model, has recently been developed and applied for the first time to the neighboring odd-Z ^{103}Nb nucleus [15]. It was demonstrated [15] that the model describes the ground state band and multi-phonon γ vibrations quite satisfactorily, supporting the interpretation of the data as one of the few experimentally known examples of the simultaneous occurrence of one- and two-phonon γ-vibrational bands. The theoretical work also generalized the well-known concept of the surface γ oscillation in deformed nuclei built on the ground state in even-even systems to γ bands based on qp configurations in odd-mass systems.

TABLE II. The systematic comparisons of the band-head energies of the 0γ, 1γ, and 2γ bands and the ratios of $(E_{2\gamma}-E_{0\gamma})/(E_{1\gamma}-E_{0\gamma})$ in ^{105}Nb with those in ^{103}Nb [12], ^{104,105,106,108}Mo [1–6,11], ^{107,109}Tc [13,14], and ^{108,110,112,114}Ru [7–10].

Nucleus	$E_{0\gamma}$	$E_{1\gamma}$ (keV)	$E_{2\gamma}$ (keV)	$\frac{(E_{2\gamma}-E_{0\gamma})}{(E_{1\gamma}-E_{0\gamma})}$
^{103}Nb	0.0	716.8	1282.1	1.79
^{105}Nb	0.0	625.9	1231.9	1.97
^{104}Mo	0.0	812.1	1583.3	1.95
^{105}Mo	0.0	870.5	1534.6	1.76
^{106}Mo	0.0	710.4	1434.6	2.02
^{108}Mo	0.0	586.1	1422.4	2.43
^{107}Tc	137.5	766.2	1499.5	2.17
^{109}Tc	69.6	633.4	1384.2	2.33
^{108}Ru	0.0	708.6	1644.8	2.32
^{110}Ru	0.0	612.7	1618.4	2.64
^{112}Ru	0.0	523.6	1413.6	2.70
^{114}Ru	0.0	563.3	1578.0	2.80

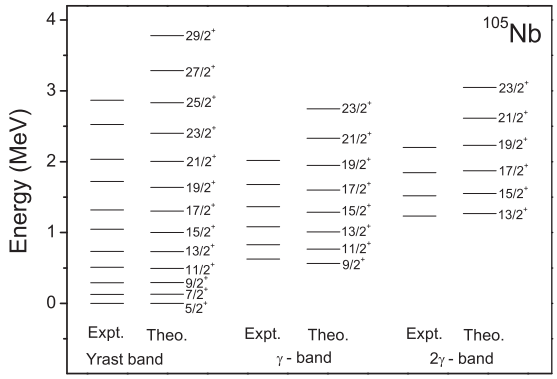

FIG. 8. Comparison of the calculated energy levels for ^{105}Nb with the experimental data.

A TPSM calculation starts with the triaxially deformed Nilsson-BCS bases. The corresponding triaxial Nilsson mean-field Hamiltonian is given by

$$\hat{H}_0 - \frac{2}{3}\hbar\omega\left[\varepsilon\hat{Q}_0 + \varepsilon'\frac{\hat{Q}_{+2}+\hat{Q}_{-2}}{\sqrt{2}}\right], \tag{14}$$

where $\hat{H}_0$ is the spherical single-particle Hamiltonian with the inclusion of appropriate spin-orbit forces parametrized by Bengtsson and Ragnarsson [36]. The model space is spanned by one- and three-qp basis

$$\hat{P}^I_{MK}a^\dagger_\pi|\Phi\rangle, \quad \hat{P}^I_{MK}a^\dagger_\pi a^\dagger_{\nu 1}a^\dagger_{\nu 2}|\Phi\rangle, \tag{15}$$

where

$$\hat{P}^I_{MK} = \frac{2I+1}{8\pi^2}\int d\Omega D^I_{MK}(\Omega)\hat{R}(\Omega) \tag{16}$$

is the three-dimensional angular-momentum projector and $|\Phi\rangle$ represents the triaxially deformed qp vacuum state. As in the projected shell model (PSM) calculations [37], we take the quadrupole-quadrupole plus pairing Hamiltonian with inclusion of the quadrupole-pairing force

$$\hat{H} = \hat{H}_0 - \frac{1}{2}\chi\sum_\mu \hat{Q}^\dagger_\mu\hat{Q}_\mu - G_M\hat{P}^\dagger\hat{P} - G_Q\sum_\mu \hat{P}^\dagger_\mu\hat{P}_\mu. \tag{17}$$

The strength of the quadrupole-quadrupole force χ is determined in a self-consistent manner so that it is related to the deformation of the basis [37]. The monopole-pairing strength is taken to be the standard form $G_M = [20.25 \mp 16.20(N-Z)/A]/A$ with "$-$" for neutrons and "$+$" for protons. The quadrupole-pairing strength G_Q is assumed to be proportional to G_M, the proportionality constant being 0.16. For more details about the model and calculation, we refer to the previous work in Ref. [15].

TPSM calculations with the above-mentioned parameters are performed for ^{105}Nb with the fixed axial deformation $\varepsilon = 0.350$ and the triaxial one $\varepsilon' = 0.130$. The calculations indicate that the yrast band (1) in ^{105}Nb originates from the $\pi 5/2^+[422]$ Nilsson orbital with $K^\pi = 5/2^+$. The obtained energy levels compared with the experimental data are presented in Fig. 8. It can be seen that the calculation achieves an excellent agreement with the available data. Not only the band-head energies for the yrast and excited bands, but also the intervals between the levels (i.e., the moments of inertia), are well described by the calculation. This strongly supports the interpretation for bands (2) and (3) as 1γ and 2γ collective bands, respectively, built on the yrast $K^\pi = 5/2^+$ structure.

IV. SUMMARY

In the present paper, the level scheme of ^{105}Nb has been reinvestigated from the study of the prompt γ rays emitted in spontaneous fission of ^{252}Cf. The yrast band has been confirmed and assigned $K^\pi = 5/2^+$ based on the $\pi 5/2^+[422]$ configuration. Three new bands have been identified. Based on the systematics and the TPSM calculations, the bands based on the 625.9 and 1231.9 keV levels have been interpreted as $9/2$ $(K+2)$ one-phonon and $13/2$ $(K+4)$ two-phonon γ-vibrational bands, respectively. The TPSM calculations agree with the excitation energies of bands (2) and (3) very well. The evidences supporting these multi-phonon γ-vibrational bands have been discussed. Another band based on the 1686.5 keV level may be a three-phonon γ-vibrational band or a three-quasiparticle band, but needs further work.

ACKNOWLEDGMENTS

The work at Tsinghua University was supported by the National Natural Science Foundation of China under Grants No. 11175095 and No. 11275067, and by the Special Program of Higher Education Science Foundation under Grant No. 2010000211007. The work at Vanderbilt University, Lawrence Berkeley National Laboratory, and Mississippi State University was supported, respectively, by the US Department of Energy under Grants No. DE-FG05-88ER40407, No. DE-AC03-76SF00098, and No. DE-FG02-95ER40939. The work at Shanghai Jiao Tong University was supported by the National Natural Science Foundation of China (Grants No. 11135005 and No. 11075103) and by the 973 Program of China (No. 2013CB834401).

[1] A. Guessous *et al.*, Phys. Rev. Lett. **75**, 2280 (1995).
[2] A. Guessous *et al.*, Phys. Rev. C **53**, 1191 (1996).
[3] L. M. Yang *et al.*, Chin. Phys. Lett. **18**, 24 (2001).
[4] R. Q. Xu *et al.*, Chin. Phys. Lett. **19**, 180 (2002).
[5] H. Hua, C. Y. Wu, D. Cline, A. B. Hayes, R. Teng, R. M. Clark, P. Fallon, A. Goergen, A. O. Macchiavelli, and K. Vetter, Phys. Rev. C **69**, 014317 (2004).
[6] H. B. Ding *et al.*, Chin. Phys. Lett. **24**, 1517 (2007).
[7] X. L. Che *et al.*, Chin. Phys. Lett. **21**, 1904 (2004).
[8] S. J. Zhu *et al.*, Int. J. Mod. Phys. E **18**, 1717 (2009).
[9] X. L. Che *et al.*, Chin. Phys. Lett. **23**, 328 (2006).
[10] E. Y. Yeoh *et al.*, Phys. Rev. C **83**, 054317 (2011).
[11] H. B. Ding *et al.*, Phys. Rev. C **74**, 054301 (2006).
[12] J. G. Wang *et al.*, Phys. Lett. B **675**, 420 (2009).
[13] L. Gu *et al.*, Chin. Phys. Lett. **26**, 092502 (2009).
[14] L. Gu *et al.*, Chin. Phys. Lett. **27**, 062501 (2010).

[15] J. A. Sheikh, G. H. Bhat, Y. Sun, and R. Palit, Phys. Lett. B **688**, 305 (2010).
[16] M. Matsuzaki, Phys. Rev. C **83**, 054320 (2011).
[17] M. A. C. Hotchkis *et al*., Nucl. Phys. A **530**, 111 (1991).
[18] Y. X. Luo *et al*., J. Phys. G: Nucl. Part. Phys. **31**, 1303 (2005).
[19] J. H. Hamilton, A. V. Ramayya, S. J. Zhu, G. M. Ter-Akopian, Yu. Ts. Oganessian, J. D. Cole, J. O. Rasmussen, and M. A. Stoyer, Prog. Part. Nucl. Phys. **35**, 635 (1995).
[20] D. C. Radford, Nucl. Instrum. Methods Phys. Res. A **361**, 297 (1995).
[21] Y. X. Luo *et al*., Nucl. Phys. A **818**, 121 (2009).
[22] S. J. Zhu *et al*., Phys. Rev. C **59**, 1316 (1999).
[23] J. K. Hwang *et al*., Phys. Rev. C **58**, 3252 (1998).
[24] S. Frauendorf, Phys. Lett. B **100**, 219 (1981).
[25] S. Frauendorf and F. R. May, Phys. Lett. B **125**, 245 (1983).
[26] F. R. Xu, W. Satula, and R. Wyss, Nucl. Phys. A **669**, 119 (2000).
[27] A. Bohr and B. R. Mottelson, *Nuclear Structure* (Benjamin, Reading, MA, 1975), Vol. 2.
[28] H. Mach, F. K. Wohn, M. Moszyǹski, R. L. Gill, and R. F. Casten, Phys. Rev. C **41**, 1141 (1990).
[29] R. A. Meyer, E. Monnand, J. A. Pinston, F. Schussler, I. Ragnarsson, B. Pfeiffer, H. Lawin, G. Lhersonneau, T. Seo, and K. Sistemich, Nucl. Phys. A **439**, 510 (1985).
[30] X. Wu, A. Aprahamian, J. Castro-Ceron, and C. Baktash, Phys. Lett. B **316**, 235 (1993).
[31] H. G. Börner, J. Jolie, S. J. Robinson, B. Krusche, R. Piepenbring, R. F. Casten, A. Aprahamian, and J. P. Draayer, Phys. Rev. Lett. **66**, 691 (1991).
[32] P. E. Garrett, M. Kadi, M. Li, C. A. McGrath, V. Sorokin, M. Yeh, and S. W. Yates, Phys. Rev. Lett. **78**, 4545 (1997).
[33] M. Oshima, T. Morikawa, Y. Hatsukawa, S. Ichikawa, N. Shinohara, M. Matsuo, H. Kusakari, N. Kobayashi, M. Sugawara, and T. Inamura, Phys. Rev. C **52**, 3492 (1995).
[34] J. A. Sheikh and K. Hara, Phys. Rev. Lett. **82**, 3968 (1999).
[35] Y. Sun, K. Hara, J. A. Sheikh, J. G. Hirsch, V. Velázquez, and M. Guidry, Phys. Rev. C **61**, 064323 (2000).
[36] T. Bengtsson and I. Ragnarsson, Nucl. Phys. A **436**, 14 (1985).
[37] K. Hara and Y. Sun, Int. J. Mod. Phys. E **4**, 637 (1995).